ACADEMIC PRESS

Available online at www.sciencedirect.com

SCIENCE DIRECT®

VIROLOGY

Virology 313 (2003) 435–451

www.elsevier.com/locate/yviro

The presence of the casein kinase II phosphorylation sites of Vpu enhances the CD4$^+$ T cell loss caused by the simian–human immunodeficiency virus SHIV$_{KU\text{-}1bMC33}$ in pig-tailed macaques

Dinesh K. Singh,[a,1] Darcy M. Griffin,[a,1] Erik Pacyniak,[a] Mollie Jackson,[a] Michael J. Werle,[a] Bo Wisdom,[b] Francis Sun,[c] David R. Hout,[a] David M. Pinson,[d] Robert S. Gunderson,[e] Michael F. Powers,[e] Scott W. Wong,[e] and Edward B. Stephens[a,*]

[a] *Department of Anatomy and Cell Biology, University of Kansas Medical Center, Kansas City, KS 66160, USA*
[b] *Department of Biochemistry and Molecular Biology, University of Kansas Medical Center, Kansas City, KS 66160, USA*
[c] *Laboratory Animal Resources, University of Kansas Medical Center, Kansas City, KS 66160, USA*
[d] *Laboratory Medicine and Pathology, University of Kansas Medical Center, Kansas City, KS 66160, USA*
[e] *Vaccine and Gene Therapy Institute, Oregon National Primate Research Center, Oregon Health and Sciences University, Beaverton, OR 97003, USA*

Received 13 December 2002; returned to author for revision 25 February 2003; accepted 31 March 2003

Abstract

The simian–human immunodeficiency virus (SHIV)/ macaque model for human immunodeficiency virus type 1 has become a useful tool to assess the role of Vpu in lentivirus pathogenesis. In this report, we have mutated the two phosphorylated serine residues of the HIV-1 Vpu to glycine residues and have reconstructed a SHIV expressing this nonphosphorylated Vpu (SHIV$_{S52,56G}$). Expression studies revealed that this protein was localized to the same intracellular compartment as wild-type Vpu. To determine if this virus was pathogenic, four pig-tailed macaques were inoculated with SHIV$_{S52,56G}$ and virus burdens and circulating CD4$^+$ T cells monitored up to 1 year. Our results indicate that SHIV$_{S52,56G}$ caused rapid loss in the circulating CD4$^+$ T cells within 3 weeks of inoculation in one macaque (CC8X), while the other three macaques developed no or gradual numbers of CD4$^+$ T cells and a wasting syndrome. Histological examination of tissues revealed that macaque CC8X had lesions in lymphoid tissues (spleen, lymph nodes, and thymus) that were typical for macaques inoculated with pathogenic parental SHIV$_{KU\text{-}1bMC33}$ and had no lesions within the CNS. To rule out that macaque CC8X had selected for a virus in which there was reversion of the glycine residues at positions 52 and 56 to serine residues and/or compensating mutations occurred in other genes associated with CD4 down-regulation, sequence analysis was performed on amplified *vpu* sequences isolated from PBMC and from several lymphoid tissues at necropsy. Sequence analysis revealed a reversion of the glycine residues back to serine residues in this macaque. The other macaques maintained low virus burdens, with one macaque (P003) developing a wasting syndrome between months 9 and 11. Histological examination of tissues from this macaque revealed a thymus with severe atrophy that was similar to that of a previously reported macaque inoculated with a SHIV lacking *vpu* (Virology 293, 2002, 252). Sequence analysis revealed no reversion of the glycine residues in the *vpu* sequences isolated from this macaque. These results contrast with those from four macaques inoculated with the parental pathogenic SHIV$_{KU\text{-}1bMC33}$, all of which developed severe CD4$^+$ T cell loss within 1 month after inoculation. Taken together, these results indicate that casein kinase II phosphorylation sites of Vpu contributes to the pathogenicity of the SHIV$_{KU\text{-}1bMC33}$ and suggest that the SHIV$_{KU\text{-}1bMC33}$/pig-tailed macaque model will be useful in analyzing amino acids/domains of Vpu that contribute to the pathogenesis of HIV-1.

Introduction

Viral protein U (Vpu) is a small transmembrane protein that is encoded by human immunodeficiency virus type 1 (HIV-1) and is synthesized off a bicistronic mRNA that also codes for the HIV-1 envelope glycoprotein (Schwartz et al., 1990). Previous studies have shown that Vpu is localized to the rough endoplasmic reticulum/Golgi complex and has several functions in the virus replication cycle (Kimura et al., 1994). Vpu has been shown to interact with newly synthesized CD4, re-translocate this molecule across the RER membrane, and target it for destruction via the protea-

* Corresponding author. Fax: +1-913-588-2710.
E-mail address: estephen@kumc.edu (E.B. Stephens).
[1] Both authors contributed equally to these studies.

0042-6822/03/$ – see front matter © 2003 Elsevier Science (USA). All rights reserved.
doi:10.1016/S0042-6822(03)00339-8

some pathway (Fujita et al., 1997; Schubert et al., 1998). Certain highly conserved domains have been shown to be essential to Vpu-mediated CD4 down-regulation. Previous studies in our laboratory have indicated that certain protein domains of Vpu are highly conserved in all strains examined (McCormick-Davis et al., 2000a). The most extensively studied of these domains is the hinge region containing the two casein kinase II phosphorylation sites and previous studies have shown that phosphorylation of both of these serine residues (at positions 52 and 56) are essential for CD4 down-regulation and are highly conserved in group M and O HIV-1 isolates (Paul and Jabbar, 1997; Raja and Jabbar, 1997; McCormick-Davis et al., 2000a). In addition to CD4 down-regulation from the surface, Vpu has also been shown to facilitate virion release from infected cells and this property of Vpu has been associated with the transmembrane domain which has been reported to have an ion channel activity (Ewart et al., 1996; Schubert et al., 1996b; Sansom et al., 1998).

While studies have established the role of the phosphoserines in CD4 degradation in cell culture studies, no studies have examined the function of the casein kinase II sites in the a relevant animal model of $CD4^+$ T cell loss. The simian–human immunodeficiency virus (SHIV) is a chimeric virus that contains the *tat, rev, vpu,* and *env* genes in a genetic background of $SIV_{mac}239$. We and others have developed pathogenic SHIVs that are capable of causing massive $CD4^+$ T cell loss and AIDS in both pig-tailed and rhesus macaques (Joag et al., 1996; Reimann et al., 1996; Luciw et al., 1999; Stephens et al., 2002). Since Vpu is found only in HIV-1 and SIVcpz (McCormick-Davis et al., 2000a), the pathogenic SHIVs have enormous potential in examining the role of Vpu in the pathogenesis in the context of a macaque model system. Previously, we have constructed a pathogenic molecular clone of SHIV known as $SHIV_{KU\text{-}1bMC33}$, which has an intact *vpu* gene and encodes for functional Vpu protein (McCormick-Davis et al., 2000b; Stephens et al., 2002). In the present study, we examined the role of casein kinase II phosphorylation of two conserved serine residues on the pathogenesis of $SHIV_{KU\text{-}1bMC33}$ in pig-tailed macaques. Our results indicate that the two casein kinase II phosphorylation sites of Vpu contribute to the pathogenicity $SHIV_{KU\text{-}1bMC33}$/pig-tailed macaque model of $CD4^+$ T cell loss and provide additional evidence that this protein enhances the pathogenicity of HIV-1. Thus, this is the first report showing a role for these sites in vivo.

Results

The VpuEGFP protein

To determine if the VpuEGFP fusion protein had a M_r that was comparable with previous reports, human 293 cells were transfected and at 48 h either radiolabeled for immune precipitation studies or examined by confocal fluorescence microscopy. Immune precipitation analysis revealed that following transfection of 293 cells with pc*vpu*EGFP, a protein with a M_r of approximately 43 kDa, was immune precipitated using a polyclonal EGFP antibody (Fig. 1). Transfection of cells with pcEGFP resulted in a protein with a M_r of approximately 27,000 (data not shown). As previous studies have reported that the size of the virus expressed protein had a M_r of 16,000, the finding of the protein with an M_r of 43,000 is close to what would be expected for the size of the fusion protein. Virus-expressed Vpu has been shown to be phosphorylated by casein kinase II and this phosphorylation has been shown to be essential to CD4 down-regulation. We determined if the VpuEGFP protein was phosphorylated by generating a site-directed mutant in which the two serine residues at positions 52 and 56 were changed to glycine residues. This plasmid, pc$vpu_{S52,56G}$EGFP, was transfected into 293 cells and radiolabeled, and the expressed protein immune precipitated from cell lysates. As shown in Fig. 1A, the M_r of the $Vpu_{S52,56G}$EGFP protein was slightly faster when compared to the intact VpuEGFP, providing indirect evidence that this protein was phosphorylated. To confirm that the VpuEGFP was phosphorylated, cells were transfected with pcEGFP, pc*vpu*EGFP, or pc$vpu_{S52,56G}$EGFPand at 48 h metabolically

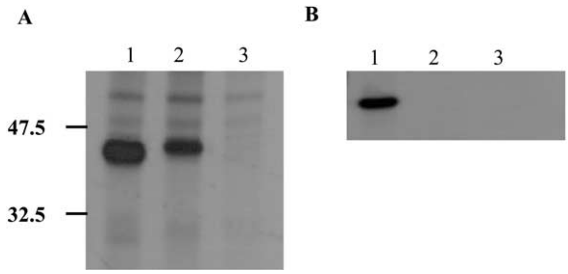

Fig. 1. Alteration of the casein kinase II phosphorylation sites results in altered mobility and a lack of phosphorylation of the VpuEGFP fusion protein. The two phosphorylated serine residues of Vpu were changed to glycine residues using site-directed mutagenesis techniques as described under Materials and Methods. (A) 293 cells were transfected with pc*vpu*EGFP, pc$vpu_{S52,56G}$EGFP, or pcDNA3.1(+) vectors as described in the text. At 48 h, cells were starved for methionine and cysteine and radiolabeled for 12 h with [^{35}S]methione/cysteine. Cells were processed and EGFP containing proteins immune precipitated using an α-EGFP serum and analyzed by SDS–PAGE as described. Lane 1, EGFP proteins immune precipitated from pc$vpu_{S52,56G}$EGFP-transfected cells; lane 2, EGFP proteins immune precipitated from pc*vpu*EGFP- transfected cells; lane 3, EGFP proteins immune precipitated from pcDNA3.1(+)-transfected cells; sizes of molecular weight markers are shown to the side of the gel. (B) 293 cells were transfected with pc*vpu*EGFP, pc$vpu_{S52,56G}$EGFP, or pcEGFP as described under Material and Methods. At 48 h, cells were washed and metabolically labeled in phosphate-free medium for 5 h with [^{32}P]orthophosphate. Cells were processed and EGFP containing proteins immune precipitated using an α-EGFP serum and analyzed by SDS–PAGE as described. Lane 1, EGFP proteins immune precipitated from pc*vpu*EGFP-transfected cells; lane 2, EGFP proteins immune precipitated from pc$vpu_{S52,56G}$EGFP-transfected cells; lane 3, EGFP proteins immune precipitated from pcDNA3.1(+)-transfected cells.

labeled with [^{32}P]-orthophosphate. Cells were washed and lysed and EGFP containing proteins immune precipitated using a polyclonal EGFP antibody. As shown in Fig. 1B, ^{32}P-labeled VpuEGFP proteins were only immune precipitated from cultures transfected with pc*vpu*EGFP, providing direct evidence that the VpuEGFP protein was phosphorylated at the casein kinase II sites.

A Vpu protein with the casein kinase II sites is localized to the same intracellular compartment in cells

We used the vectors expressing the VpuEGFP and $Vpu_{S52,56G}$EGFP to analyze intracellular localization. When transfected into 293 cells, the wild-type VpuEGFP protein was localized to RER/Golgi complex compartments and was not observed on the cell surface to any significant extent, similar to the reported findings for the virus-expressed protein (Kimura et al., 1994). Expression of the $Vpu_{S52,56G}$EGFP in this expression system is shown in Fig. 2 and shows that the $Vpu_{S52,56G}$EGFP protein had the same intracellular localization as the unmodified VpuEGFP protein, demonstrating that the casein kinase II sites were not required for Vpu targeting to the RER/Golgi compartments.

A Vpu protein with the casein kinase II sites prevents CD4 expression on the cell surface

Using the VpuEGFP reporter, we also analyzed the ability of $Vpu_{S52,56G}$EGFP to prevent CD4 expression on the cell surface. As shown in Figs. 3A–D, HeLa CD4$^+$ cells transfected with the VpuEGFP vector clearly abolished cell surface expression of CD4 (Table 1). In contrast, transfection of cultures with the pc*vpu*$_{S52,56G}$EGFP vector still resulted in the expression of CD4 on the cell surface and was similar to cultures transfected with pcEGFP, which expresses only EGFP reporter protein (Table 1). These results indicate that mutation of the serine residues at positions 52 and 56 to glycine residues abolished the ability of Vpu to prevent CD4 from being expressed on the cell surface.

Inoculation of four pig-tailed macaques with $SHIV_{KU\text{-}1bMC33}$ resulted in a rapid loss of circulating CD4$^+$ T cells in four of four pig-tailed macaques

All four macaques inoculated with parental $SHIV_{KU\text{-}1bMC33}$ exhibited a severe loss in their circulating CD4$^+$ T cells by 1 month postinoculation that was maintainedthroughout the course of their 6-month infection (Fig. 4A). Examination of the plasma virus loads from two of these macaques (CM4G and CM4K) revealed a high number of viral copies in the plasma early after inoculation, which was maintained above 10,000 copies throughout the course of their 6-month infection (Fig. 4B). Histological examination of tissues at necropsy revealed the typical lymphoid depletion in the thymus, spleen, and lymph nodes that is associated with pathogenic $SHIV_{KU\text{-}1bMC33}$ infection (Stephens et al., 2002). Examination of visceral organs for viral sequences revealed that eight of nine visceral organs were positive for viral *gag* sequences from macaques CM4G and CM4K (data not shown) and that amplification of 2-LTR circles, indicative of recent infection, revealed that six of nine visceral organs were positive (Fig. 4C). Histological examination of 15 regions of the CNS from these four macaques revealed no lesions consistent with lentiviral encephalitis. Of the 15 regions of the CNS examined from macaques CM4G and CM4K, no regions and 1 region were positive for 2-LTR sequences, respectively (data not shown), indicating that the virus was poorly neuroinvasive in these macaques.

Table 1
Results of transfection of HeLa CD4$^+$ cells with vectors expressing EGFP, VpuEGFP, or $Vpu_{S52,56G}$EGFP on cell surface CD4 expression

	Vector		
	EGFP	VpuEGFP	$Vpu_{S52,56G}$EGFP
% HeLa cells positive for CD4	85	81	79
% HeLa cell positive for EGFP expression	20	10%	12%
% HeLa cells positive for EGFP cell surface CD4 expression[a]	100	0%	100%

[a] Number of EGFP, VpuEGFP, or $Vpu_{S52,56G}$EGFP expressing HeLa CD4$^+$ cells counted from three experiments exceeded 400.

Inoculation of four pig-tailed macaques with $SHIV_{S52,56G}$ resulted in a rapid loss of circulating CD4$^+$ T cells in one of four pig-tailed macaques

We determined whether the $SHIV_{S52,56G}$ replicated with the same kinetics as the parental $SHIV_{KU\text{-}1bMc33}$. Equivalent amounts of each virus were used to inoculate C8166 cultures and culture supernatants assayed for p27 over a 10-day period. The $SHIV_{S52,56G}$ virus replicated with similar kinetics as the parental $SHIV_{KU\text{-}1bMC33}$ (data not shown). We next inoculated four pig-tailed macaques (CC8X, CC8V, P003, and P017) with $SHIV_{S52,56G}$. The circulating CD4$^+$ T cell numbers and plasma virus loads following inoculation are shown in Figs. 5A and B. Macaque CC8X developed a severe loss in its circulating CD4$^+$ T cells soon after inoculation (15 cells/1 by 4 weeks postinoculation) and this loss was maintained throughout the course of the 18-week infection. The severe loss of CD4$^+$ T cells in this macaque was similar to that in macaques inoculated with the unmodified $SHIV_{KU\text{-}1bMC33}$ (Fig. 4). Examination of plasma viral loads by real time RT–PCR revealed that the macaque CC8X had the highest viral loads throughout the course of the infection with $SHIV_{S52,56G}$. At necropsy, histological examination of the tissues revealed severe lymphoid deple-

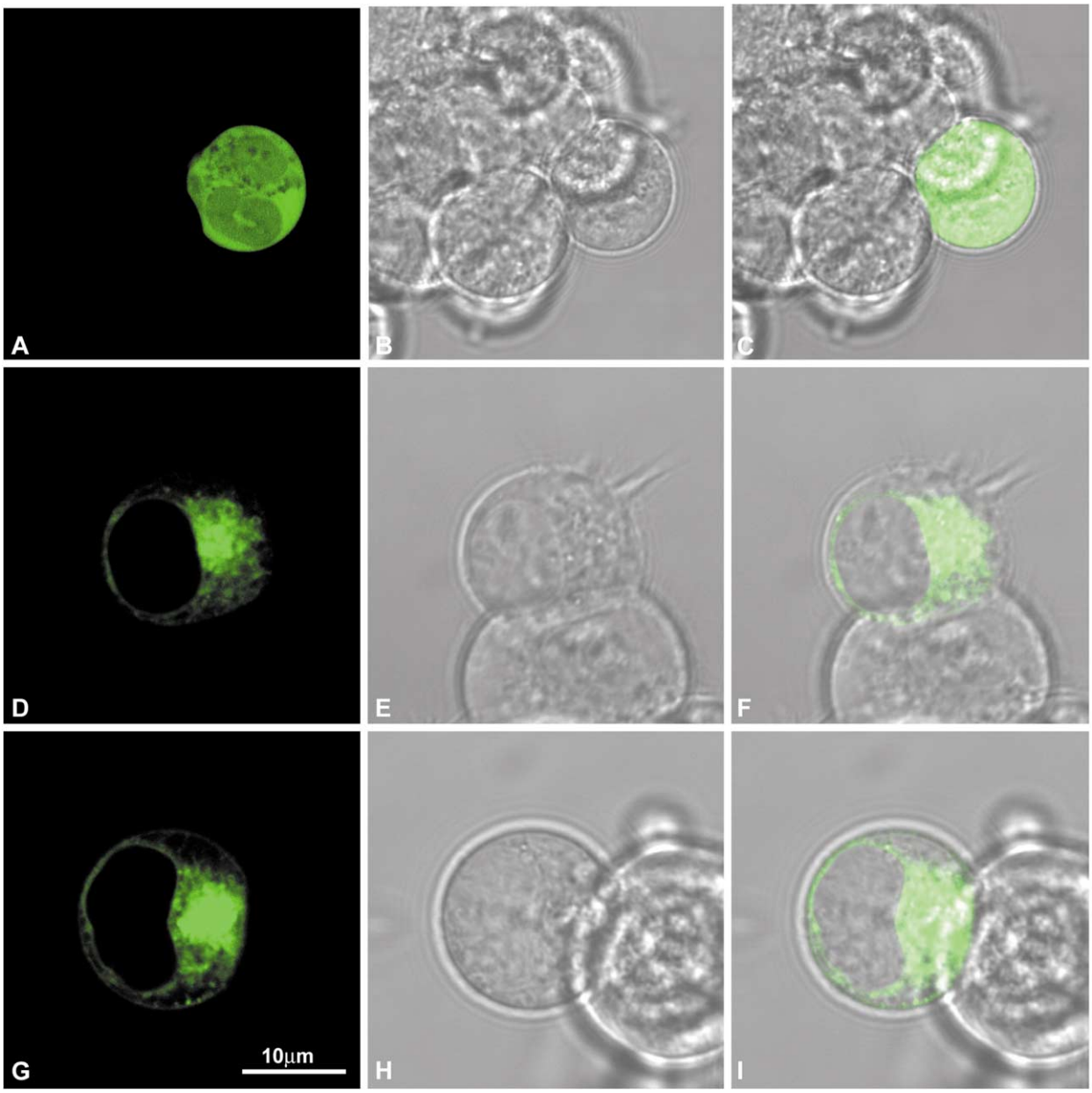

Fig. 2. The $Vpu_{S52,56G}$EGFP is localized to the same intracellular compartment as the unmodified VpuEGFP. 293 cells were transfected with pcEGFP, pc*vpu*EGFP, and pc$vpu_{S52,56G}$EGFP vectors as described in the text and at 48 h examined by fluorescence confocal (A, D, and G), phase–contrast (B, E, and H) microscopy. Panels C, F, and I merge the confocal and phase–contrast images. (A–C) 293 cells transfected with pcEGFP. (D–F) 293 cells transfected with pc*vpu*EGFP. (H and I) 293 cells transfected with $vpu_{S52,56G}$EGFP.

tion in thymus, spleen, and lymph nodes of CC8X (Fig. 6), which is typical of pig-tailed macaques inoculated with pathogenic $SHIV_{KU\text{-}1bMC33}$. Examination of 14 regions of the CNS from CC8X revealed no lesions consistent with lentiviral encephalitis. Examination of tissue DNAs from CC8X using PCR that amplified the viral *gag* revealed that eight of eight visceral organs were positive (data not shown) and amplification of 2-LTR circles, indicative of recent infection, was detected in six of ten visceral organs, with only the heart, kidney, liver, and pancreas negative (Fig. 7). Of the 14 regions of the CNS examined, only 3 regions were positive for *gag* sequences (motor cortex, parietal cortex, and midbrain), with the midbrain also being positive for the presence of 2-LTR circle sequences (data not shown), indicating that the virus was poorly neuroinvasive in this macaque.

The serine to glycine changes in vpu were not stable throughout the course of infection of macaque CC8X

Because of the severe loss of $CD4^+$ T cells in CC8X, one possibility was that there was a selection for mutations in

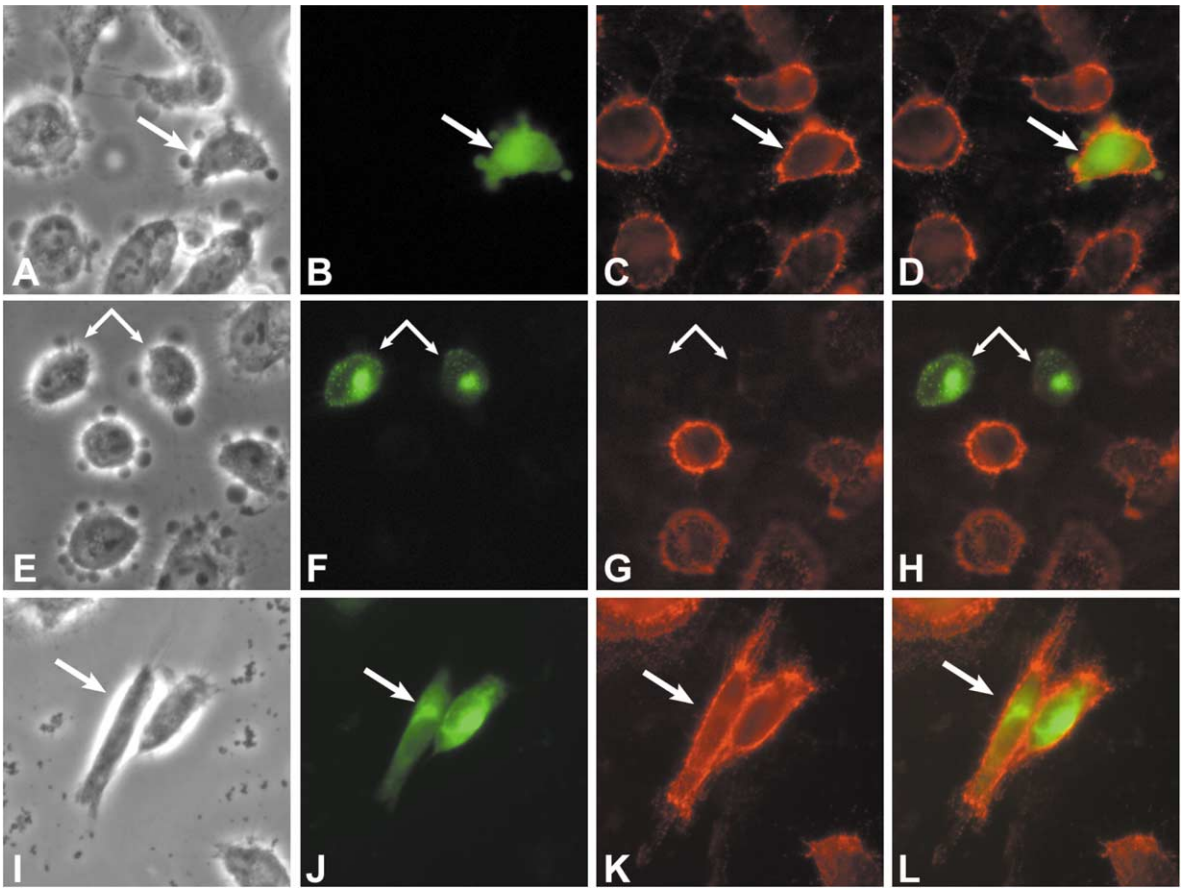

Fig. 3. The $Vpu_{S52,56G}$EGFP is does not prevent CD4 from being expressed on the cell surface. HeLa $CD4^+$ cells, which express CD4, were transfected with pcEGFP, pc*vpu*EGFP, or pc$vpu_{S52,56G}$EGFP vectors. At 48 h posttransfection, cells were stained for surface CD4 using α-CD4-RITC antibody followed by fixation with 1% formalin. Cells were analyzed by phase–contrast microscopy (A,E, and I) or fluorescence microscopy using a fluorescein filter (indicating VpuEGFP expression; B,F, and J) or a rhodamine filter (for CD4 surface expression; C, G, and K) or dual filters (for expression of VpuEGFP and CD4 expression; D, H, and L). (A–D) Transfection with the pcEGFP construct. (E–H) Transfection with the pc*vpu*EGFP construct. (I–L) Transfection with the pc$vpu_{S52,56G}$EGFP construct.

the *vpu* that resulted in the reversion of the glycine residues at positions 52 and 56 back to serine residues. In order to test this hypothesis, *vpu* was amplified by PCR from PBMC DNA isolated at 3, 8, and 12 weeks and at necropsy (18 weeks) from macaque CC8X and directly sequenced. The bulk PCR sequencing results were confirmed for CC8X and CC8V by cloning and sequencing individual *vpu* clones. In addition, we also examined the *vpu* sequences from the mesenteric lymph node, thymus and spleen tissues at necropsy. The results of the sequence analysis are shown in Figs. 8A and B. Direct sequence analysis of *vpu* amplified from PBMC DNA by nested PCR revealed that the glycine change at position 52 was stable at 3 weeks postinoculation. Direct sequence analysis of *vpu* amplified from PBMC DNA at 3 weeks revealed the presence of an A (which would code for a serine at position 56) and G (coding for the input glycine the same position) at position 169 of the gene. However, this was not confirmed by sequencing of individual *vpu* clones. At 8 weeks, direct sequencing of PCR products and individual *vpu* clones revealed changes at both position 157 (G to A resulting in a serine) and position 169. These results were also seen at 12 and 18 weeks (necropsy) and confirmed in the analysis of *vpu* genes in the spleen, lymph nodes, and thymus. In order to rule out that this macaque might have been inoculated with a stock that was contaminated with the parental $SHIV_{KU\text{-}1bMC33}$, the *vpu* gene in the virus stocks used to inoculate the macaques was extensively analyzed. Only the *vpu* gene coding for glycines at positions 52 and 56 was found. Sequence analysis of the PBMC and lymphoid tissues from the other three macaques did not reveal the reversions observed with CC8X.

The glycine to serine reversions were found in viruses recovered from infectious viruses recovered from macaque CC8X

As we were able to detect reversions in *vpu* at later times after inoculation by amplification of the gene from tissue DNAs, we determined if these reversions were present in viruses recovered from various organs at necropsy. Culture supernatants were recovered by cocultures of cells isolated from the PBMC, thymus, spleen, and mesenteric lymph

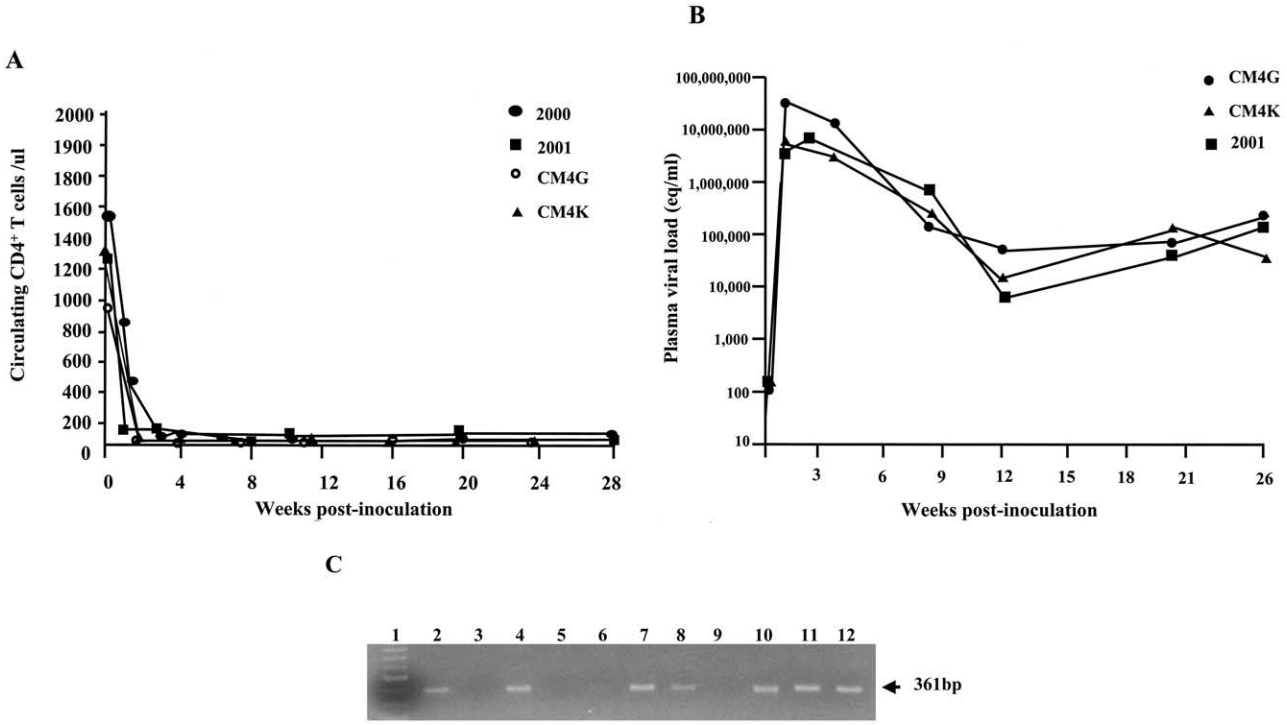

Fig. 4. $SHIV_{KU\text{-}1bMC33}$ was pathogenic for four of four macaques 2000 (●), 2001 (■), CM4G (○), and CM4K (▲). (A) Macaques were inoculated with $SHIV_{KU\text{-}1bMC33}$ and circulating $CD4^+$ T cells determined at various times postinoculation. (B) Virus RNA levels were performed on RNA extracted from 500 liters of EDTA-treated plasma. Samples were subjected to real-time RT–PCR and Taqman probe homologous to the SIV *gag* gene. Standard curves were generated using five dilutions of viral RNA of known concentration. (C) Viral 2-LTR sequences were amplified using PCR from DNA samples from visceral organs from macaque CM4K. The order of the gels is shown in C: lane 1, molecular weight markers (100 bp); lane 2, positive control—lymph node of macaque 50O; lane 3, negative control—lymph node from an uninoculated macaque; lane 4, lung; lane 5, liver; lane 6, kidney; lane 7, axillary lymph node; lane 8, mesenteric lymph node; lane 9, pancreas; lane 10, small intestine; lane 11, spleen; lane 12, thymus.

nodes with C8166 cells. The harvested supernatants were filtered and used to inoculate fresh C8166 cultures. The cells from these cultures were harvested at 4 days postinoculation, the DNA was isolated, and the *vpu* gene amplified. Sequence analysis of the PCR products indicated that the reversions at both positions in *vpu* could be detected in the viruses isolated from the PBMC, lymph node, and spleen but not in virus isolated from the thymus (Fig. 8B). Virus harvested from CC8V, P017, and P003 at necropsy maintained glycine residues at positions 52 and 56.

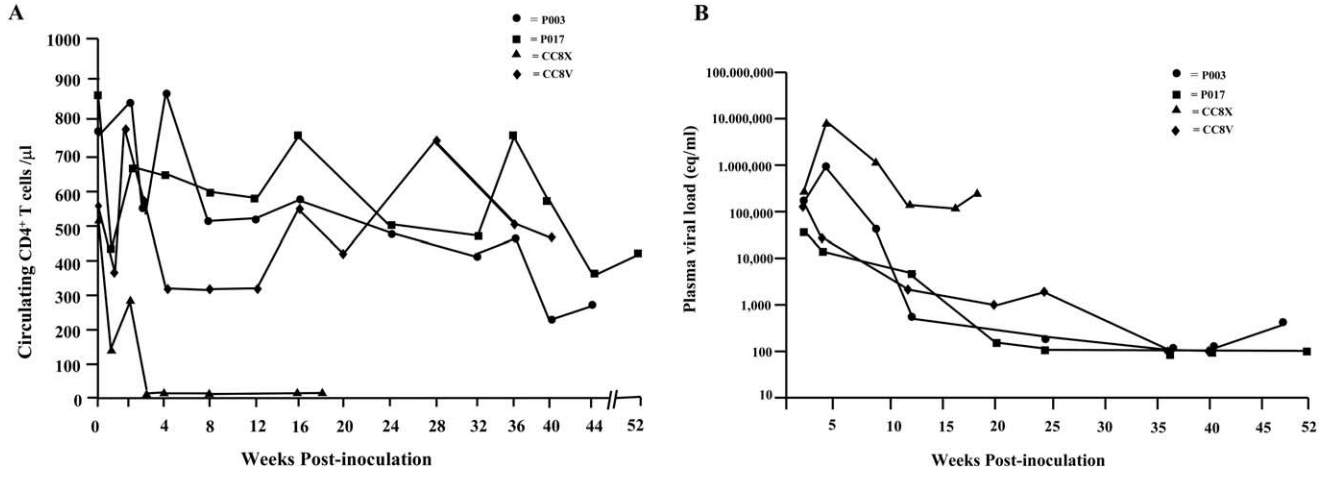

Fig. 5. Circulating $CD4^+$ T cells and plasma virus loads following inoculation of pig-tailed macaques with $SHIV_{S52,56G}$. (A) The levels of circulating $CD4^+$ T cells in macaques CC8X (▲), CC8V (◆), P003 (●), and P017 (■) following inoculation with $SHIV_{S52,56G}$. (B) The plasma virus loads in macaques CC8X (▲), CC8V (◆), P003 (●), and P017 (■) following inoculation with $SHIV_{S52,56G}$.

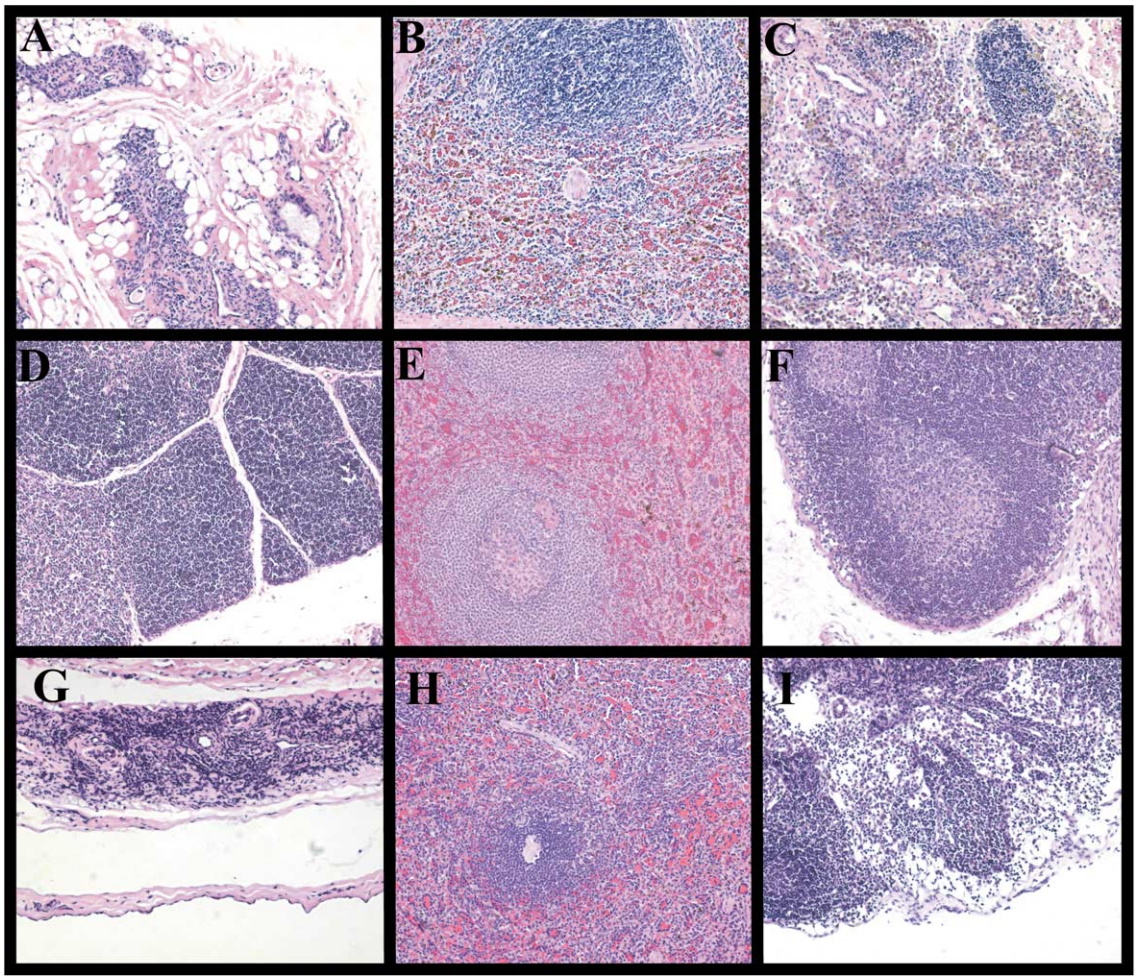

Fig. 6. Histopathology of macaques CC8X, CC8V, and P003. Micrographs of thymus (A,D, and G), spleen (B, E, and H), and mesenteric lymph node (C, F, and I) showing histological changes. (A–C) Macaque CC8X. (D–F) Macaque CC8V. (G–I) Macaque P003. Examination of the spleen, lymph nodes, and thymus from macaques inoculated with parental $SHIV_{KU\text{-}1bMC33}$ revealed lesions similar to that observed with macaque CC8X.

Compensating mutations in Env and Nef were not observed after inoculation with $SHIV_{S52,56G}$

Another possibility that had to be considered was that because of the mutations engineered in *vpu*, virus might have been selected for mutations in other viral genes involved in CD4 down-regulation, namely, *env* and *nef*, that would have compensated for the lack of a functional Vpu.

We amplified, cloned, and sequenced the gp120 and Nef regions of the viral genome from PBMCs at 3, 8, and 18 weeks as well as from lymph node and spleen tissue at necropsy. The results of the sequence analysis indicated that at necropsy, there were no consensus amino acid substitutions in either the gp120 or *nef* genes, which was the time when CC8X had developed a massive loss of circulating $CD4^+$ T cells (data not shown).

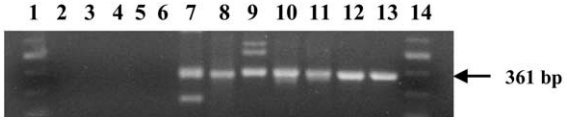

Fig. 7. Distribution of virus in macaque CC8X. Viral 2-LTR sequences were amplified using PCR from DNA samples from visceral organs, from macaque CC8X. The order of the gels shown is as follows: lane 1, molecular weight markers (100 bp); lane 2, negative control—lymph node from an uninoculated macaque; lane 3, heart; lane 4, kidney; lane 5, liver; lane 6, pancreas; lane 7, lung; lane 8, inguinal lymph node; lane 9, mesenteric lymph node; lane 10, small intestine; lane 11, spleen; lane 12, thymus; lane 13, positive control—lymph node of macaque 50O; lane 14, molecular weight markers (100 bp).

Macaque CC8V, P003, and P017 maintained low virus burdens

In contrast to macaque CC8X, macaques CC8V, P003, and P017 did not develop a significant loss of $CD4^+$ T cells over a 9- to 11-month period following inoculation with $SHIV_{S52,56G}$ (Fig. 4A). This was also reflected in the plasma virus loads when compared to CC8X (Fig. 4B). Macaque CC8V was sacrificed at 40 weeks postinoculation to deter-

A

```
SHIVKU-1b            MQPIPIVAIVALVVAIIIAIVVWSIVIIEYRKILRQRKIDRLIDRLIERAEDSGNESEGEISALVEMGVEMGHHATWDVDDL
SHIVS52,56G          MQPIPIVAIVALVVAIIIAIVVWSIVIIEYRKILRQRKIDRLIDRLIERAEDGGNEGEGEISALVEMGVEMGHHATWDVDDL

3 WEEKS
                                                                      S
CC8X PBMC bulk PCR   ------------------------------------------------------------------------------------
CC8XPBMC-3           ---------------------------------------------------------------------------------R-----
CC8XPBMC-4           ------------------------------------------------------------------------------------
CC8XPBMC-7           ------------------------------------------------------------------------------------
CC8XPBMC-8           ----------------------*-------------------------------------------------------------
CC8XPBMC-11          ------------------------------------------------------------------------------------

CC8V PBMC bulk PCR   ------------------------------------------------------------------------------------
CC8VPBMC-1           ------------------------------------------------------------------------------------
CC8VPBMC-4           ---------------T----------------------------------------------------------------------
CC8VPBMC-5           ------------------------------------------------------------------------------------
CC8VPBMC-9           ----------------------------------------G-------------------------------T-----------
CC8VPBMC-10          ------------------------------------------------------------------------------------

P003 PBMC bulkPCR    ------------------------------------------------------------------------------------
P017 PBMC bulkPCR    ------------------------------------------------------------------------------------


8 WEEKS
                                                                    S   S
CC8X PBMC bulk PCR   ------------------------------------------------------------------------------------
CC8XPBMC-1           ------------------------------------------------------------------------------------
CC8XPBMC-2           ----------------------------------------------------S---S------------------R-----
CC8XPBMC-4           ------------------------------------------------------------------------------------
CC8XPBMC-7           ---------------------------K----------------------------------------------------------
CC8XPBMC-10          ----------------------------------------------------S---S-------------------------

CC8V PBMC bulk PCR   ------------------------------------------------------------------------------------
CC8V PBMC-8          ------------------------------------------------------------------------------------
CC8VPBMC-12          ------------------------------------------------------------------------------------
CC8VPBMC-17          -------------------T----------------------------------------------------------------
CC8VPBMC-18          ----------------------------------------------------------K-------------------------
CC8VPBMC-22          ------------------------------------------------------------------------------------

P003 PBMC bulkPCR    ------------------------------------------------------------------------------------
P017 PBMC bulkPCR    ------------------------------------------------------------------------------------

12 WEEKS
                                                                    S   S
CC8X PBMC bulk PCR   ------------------------------------------------------------------------------------
CC8XPBMC-1           I-----------------------------------------------------------------------------------
CC8XPBMC-3           ----------------------------------------------------S---S-------------------------
CC8XPBMC-4           ------------------------------N-----N-------------S---S-------------------------
CC8XPBMC-5           ---------------------------G--------------------------------------------------------
CC8XPBMC-10          -----------------------------------N-------------S---S-------------------------

16 WEEKS

CC8VPBMC-1           ------------------------------------------------------------------------------------
CC8VPBMC-2           ------------------------------------------------------------------------------------
CC8VPBMC-7           -------------------T----------------------------------------------------------------
CC8VPBMC-8           ----------------------------------------------------------K-------------------------
CC8VPBMC-12          ------------------------------------------------------------------------------------

P003 PBMC bulk PCR   ------------------------------------------------------------------------------------
P017 PBMC bulk PCR   ------------------------------------------------------------------------------------

18 WEEKS
                                                                    S   S
CC8X PBMC bulk PCR   ------------------------------------------------------------------------------------
CC8XPBMC-6           -------V--------------G----------------------------S---S----------------------N-
CC8XPBMC-10          ----------------------------------------------------S---S-------------------------
CC8XPBMC-12          I---------------------------------------------------S---S-------------------------
CC8XPBMC-13          ------------------------------------H--------------S---S-------------------------
CC8XPBMC-14          I--------------------*-----------------------------------------------------------
CC8X PBMC VIRUS      ----------------------------------------------------S---S-------------------------
```

Fig. 8. Sequence analysis of the *vpu* gene from CC8X and CC8V reveals that the S52,56G amino acid substitutions were not stable over the course of the infection in CC8X. Shown are the predicted amino acid sequences from *vpu* genes amplified from PBMC DNA samples isolated at various time postinoculation (A) as well as from the tissue DNA samples (lymph node, spleen, and thymus) obtained at necropsy (B). Sequence ambiguities at particular positions from the bulk PCR sequencing results are shown above the sequence.

mine viral loads in various organs and to determine if virus infection resulted in histological lesions in any organs. Histological examination of the tissues from macaque CC8V revealed no lesions in any of the visceral organs examined or the CNS (Fig. 6). Examination of the visceral organs for viral 2-LTR sequences revealed that only four of nine or-

A (cont)

```
SHIVS52,56G          MQPIPIVAIVALVVAIIIAIVVWSIVIIEYRKILRQRKIDRLIDRLIERAEDGGNEGEGEISALVEMGVEMGHHATWDVDDL

P003 PBMC bulk PCR    --S----------------------------------------------------R----------------------
P017 PBMC bulkPCR    ------------------------------------------------------------------------------

28 weeks

P003 PBMC bulkPCR    ------------------------------------------------------------------------------
P017 PBMC bulkPCR    ------------------------------------------------------------------------------

31weeks

P003 PBMC bulkPCR    ----------------------------------------------------------R----------------------
P017 PBMC bulkPCR    ------------------------------------------------------------------------------

35weeks

P003 PBMC bulkPCR    ------------------------------------------------------------------------------
P017 PBMC bulkPCR    ------------------------------------------------------------------------------

39weeks

P003 PBMC bulkPCR    ----------------------------------------------------------R----------------------
P017 PBMC bulkPCR    ------------------------------------------------------------------------------

52 weeks

P017 PBMC bulk PCR   ------------------------------------------------------------------------------
```

B

```
SHIVKU-1b            MQPIPIVAIVALVVAIIIAIVVWSIVIIEYRKILRQRKIDRLIDRLIERAEDSGNESEGEISALVEMGVEMGHHATWDVDDL
SHIVS5256G           MQPIPIVAIVALVVAIIIAIVVWSIVIIEYRKILRQRKIDRLIDRLIERAEDGGNEGEGEISALVEMGVEMGHHATWDVDDL
                                                                 S  S
CC8XLN bulk PCR      ------------------------------------------------------------------------------
CC8XLN-1             --------------T---------------------------NK-K-----S--KSKKK-----K-EIK----TT|N-NN-
CC8XLN2              ----------------------*-------------------------------------------------------
CC8XLN3              ----------------------*----------------------------S---S-----------------------
CC8XLN4              ----------------------*-------------------------------------------------------
CC8XLN5              ----------------------*-----------------------------------------R--------------
CC8XLN6              ----L-----------------*-----------------------------D--E-------KIE-K------------
CC8XLN7              ----------------------*-----------------------------------------R--------------
CC8XLN18             ----------------------*----------------------------S---S-----------------------

CC8XLNVIRUS          ------------------------------------------------------S---S--K------------P---------

                                                                       S
CC8XSP bulk PCR      ------------------------------------------------------------------------------
CC8XSP2              I-----------------------------------------------------S---S-----------------------
CC8XSP11             ------------------------------------------------------S---S-----------------------
CC8XSP12             ------------------------------------------------------S---S---K----------I---------N
CC8XSP15             ------------------------------------------------------S---S-----------------------
CC8XSP18             ----------------------*-------------------------------------------------------

CC8XSPVIRUS          ------------------------------------------------------S---S-----------------------


CC8XTHY bulk PCR     ------------------------------------------------------------------------------
CC8XTHY2             ------------------------------------------------------------P-------------------
CC8XTHY5             ------------------------------------------------------S---S-----------------------
CC8XTHY7             ----------------------*-------------------------------------------------------
CC8XTHY8             ----------------------*--------------------N----------------------------------
CC8XTHY9             ----------------------*-----------------------------------------------T----------
CC8XTHY12            ---------------------------------------------G----------------------------------
CC8XTHY16            ----------------------*-------------------------------------------------------
CC8XTHY17            ------------------------T-----------------------------------------------------

CC8XTHYVIRUS         ---------------------R----------------------------------*-------------P---------

CC8V SP bulk PCR     ------------------------------------------------------------------------------
CC8V LN bulk PCR     ------------------------------------------------------------------------------
CC8V THY bulk PCR    ------------------------------------------------------------------------------

P003 SP bulk PCR     ------------------------------------------------------------------------------
P003 LN bulk PCR     ------------------------------------------------------------------------------
P003 THY bulk PCR    ------------------------------------------------------------------------------

P017 SP bulk PCR     ------------------------------------------------------------------------------
P017 LN bulk PCR     ------------------------------------------------------------------------------
P017 THY bulk PCR    ------------------------------------------------------------------------------
```

Fig. 8 (*continued*)

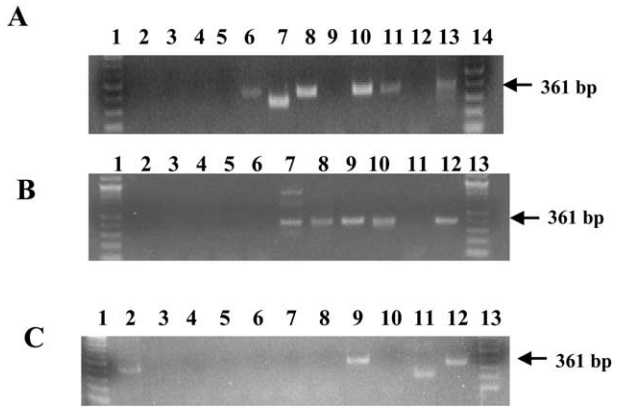

Fig. 9. Detection of 2-LTR circles in visceral organs from macaques CC8V, P003, and P017. DNA was isolated from various visceral organs and 2-LTR circles were amplified as described in the text. (A) Macaque P003. (B) Macaque CC8V. (C) Macaque P017. The order of the gel in A is as follows: lane 1, molecular weight marker (100 bp); lane 2, negative control—lymph node from an uninoculated macaque; lane 3, kidney; lane 4, liver; lane 5, lung; lane 6, axillary lymph node; lane 7, inguinal lymph node; lane 8, mesenteric lymph node; lane 9, pancreas; lane 10, small intestine; lane 11, spleen; lane 12, thymus; lane 13, positive control—lymph node of macaque 50O; lane 14, molecular weight marker (100 bp). The order of the gel in B is as follows: lane 1, molecular weight marker (100 bp); lane 2, negative control—lymph node from an uninoculated macaque; lane 3, kidney; lane 4, liver; lane 5, lung; lane 6, pancreas; lane 7, inguinal lymph node; lane 8, mesenteric lymph node; lane 9, small intestine; lane 10, spleen; lane 11, thymus; lane 12, positive control—lymph node of macaque 50O; lane 13, molecular weight marker (100 bp). The order of the gel in C is as follows: lane 1, molecular weight marker (100 bp); lane 2, positive control—lymph node of macaque 50O; lane 3, negative control—lymph node from an uninoculated macaque; lane 4, kidney; lane 5, liver; lane 6, lung; lane 7, axillary lymph node; lane 8, inguinal lymph node; lane 9, mesenteric lymph node; lane 10, spleen; lane 11, small intestine; lane 12, thymus; lane 13, molecular weight marker (100 bp).

gans (inguinal lymph node, mesenteric lymph node, small intestine, and spleen) were positive for the presence of 2-LTR sequences, respectively (Fig. 9B). The presence of replicating virus in the lymphoid organs is similar to results obtained with other SHIV viruses that failed to cause significant depletion of $CD4^+$ T cells (McCormick-Davis et al., 2000b; Stephens et al., 2002).

Beginning at 9 months postinoculation, macaque P003 started to develop a loss of appetite and a decrease in the number of circulating $CD4^+$ T cells (500 cells/μ1 at 9 months to 270 cells/μ1 at 11 months). This macaque was euthanized at 11 months in a moribund condition and virus burdens were analyzed. Virus could not be recovered from coculturing of PBMC, spleen, lymph node, or thymus cells with C8166 cells, suggesting very low virus burdens in this macaque. Histological examination of the tissues from macaque P003 revealed that mesenteric lymph nodes and thymus had undergone severe atrophy, while the spleen had no significant lesions (Fig. 6). No histological changes or opportunistic infections were observed in the heart, kidney, lung, liver, pancreas, and small intestine that might have accounted for the animal's moribund state. Examination of the visceral organs for 2-LTR sequences revealed that only five of ten organs (axillary, inguinal, and mesenteric lymph nodes, small intestine, and spleen) were positive for the presence of 2-LTR sequences, respectively (Fig. 9A). There were no histological lesions in the CNS and nested PCR did not detect *gag* or 2-LTR sequences in any region of the CNS of macaque P003 (data not shown).

Macaque P017 was euthanized in good condition at 12 months after inoculation. Virus could not be recovered from coculturing of spleen, lymph node, or thymus cells with C8166 cells, suggesting low virus burdens in this macaque. Histological examination of the tissues (heart, kidney, lungs, liver, mesenteric lymph nodes, pancreas, spleen, small intestine, and thymus) from macaque P017 revealed no significant lesions in any tissues. Examination of the visceral organs for 2-LTR sequences revealed that only three of nine organs (mesenteric lymph node, small intestine, and thymus) were positive for the presence of 2-LTR sequences, respectively (Fig. 9C). There were no lesions in the CNS and nested PCR did not detect *gag* or 2-LTR sequences in any region of the CNS of macaque P017 (data not shown).

Viral DNA loads in lymphoid tissues at necropsy correlated with disease progression

We quantified the levels of viral copies in DNA isolated from the spleen, lymph node, and thymus tissues derived from macaques CC8X, CC8V, P003, and P017 at necropsy. As shown in Fig. 10, the levels of viral copies in the spleen, lymph node, and thymus were 10 to 10,000 times higher in samples derived from macaque CC8X when compared to those from the other three macaques, CC8V, P003, or P017. The number of virus copies in the lymphoid tissues of macaque CC8X was similar to that observed in two macaques inoculated with parental $SHIV_{KU\text{-}1bMC33}$ (Fig. 10).

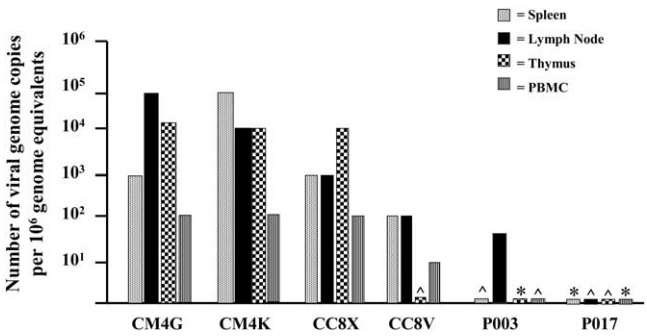

Fig. 10. Analysis of viral DNA copy loads at necropsy in macaques inoculated with and $SHIV_{KU\text{-}1bMC33}$ and $SHIV_{S52,56G}$. Total cellular DNA was extracted from the tissues and used to quantitate the number of viral copies per 10^6 genorne equivalents in the mesenteric lymph node, spleen, thymus, and PBMC as described under Materials and Methods. Values designated with (^) indicate that the *gag* sequences were detectable but less than one copy was detected per 10^6 genome equivalents and values designated with a (*) indicate that the viral *gag* was not detectable by nested DNA PCR.

Thus, these results indicated that macaque CC8X, which developed rapid $CD4^+$ T cell loss, also had had the highest viral copy numbers in lymphoid tissues.

Discussion

Studies have shown that three proteins (Env, Nef, and Vpu) of HIV-1 can interact with the CD4 molecule and some investigators have suggested that the CD4 down-regulation function of Vpu is redundant (Piquet et al., 1998). The first of the three HIV-1 proteins involved in CD4 down-regulation is the gp160 Env precursor which forms a complex with the newly synthesized CD4 molecules inside the rough endoplasmic reticulum (RER) to prevent CD4 traffic to the surface (Crise et al., 1990; Jabbar and Nayak, 1990; Bour et al., 1995). While Nef acts preferentially on cell surface CD4 (Garcia and Miller, 1991), Vpu acts on CD4 in the RER to block the trafficking of newly synthesized CD4 molecules to the cell surface membrane (Willey et al., 1990). While the formation of CD4–gp160 complexes in the ER blocks the maturation and transport of CD4 to the surface, it creates a problem for the virus as the envelope protein is also blocked from reaching the cell surface, where it is required for the assembly of infectious virions (Bour et al., 1995). It has been documented that synthesis of equimolar amounts of CD4 and Env leads to the production of noninfectious virions devoid of envelope protein, as most of the Env is attached to CD4 inside the endoplasmic reticulum and is simply not available for virion assembly at the cell surface (Buonocore et al., 1994).

Previous studies have shown that the enhancement of virion release and degradation of CD4 can be assigned to different domains of the Vpu protein. While the transmembrane domain of Vpu has been shown to be important for the enhancement of virion release, the cytoplasmic domain of Vpu has been shown to be important in CD4 degradation (Schubert et al., 1996a; Paul et al., 1998). Regarding Vpu-mediated CD4 degradation, phosphorylation of the two casein kinase II sites in the cytoplasmic domain has been shown to be essential to this function and it happens to be the most conserved sequence in Vpu proteins isolated from different subtypes of HIV-1 (Schubert et al., 1994; Paul et al., 1997; McCormick-Davis et al., 2000a). The phosphoserine residues have been shown to interact with the cytoplasmic domain of the CD4 molecule in the RER to shunt CD4 to the proteasome pathway (Fujita et al., 1997; Schubert et al., 1998). Thus, Vpu has a potential role in the pathogenesis of HIV-1 and SHIV by promoting the degradation of CD4 molecules in these complexes, allowing Env transport to the cell surface for assembly into viral particles.

Because the Vpu protein is found in HIV-1 and a limited number of SIV strains, the assessment of the role of Vpu in HIV-1 pathogenesis using the SIVmac or HIV-2/macaque models has not been possible. Our laboratory has been using the SHIV/pig-tailed macaque model system to assess the role of this gene product in lentiviral pathogenesis. We showed that during the derivation of a pathogenic variant from the nonpathogenic SHIV-4 virus that the virus had accumulated changes within several genes that were associated with its newly acquired pathogenesis. Relevant to the studies reported here, the *vpu* gene of SHIV-4 did not code for a functional Vpu as the initiation codon was ACG but had reverted during derivation of a pathogenic virus (Stephens et al., 1997; McCormick-Davis et al., 1998). Subsequently, we developed a molecular clone of one of these pathogenic variants that caused $CD4^+$ T cell loss and AIDS in pig-tailed macaques. Using this clone, we constructed a virus (*vpu*$SHIV_{KU\text{-}1bMC33}$) in which that deletion of the majority of *vpu* such that the expressed protein was nonfunctional resulted in disease only in one of four macaques inoculated (McCormick-Davis et al., 2000b). We showed that the virus from the one macaque that developed neuroAIDS had accumulated additional changes in *nef* and *env* that probably compensated for the lack of a functional *vpu* gene, whereas the virus isolated from macaques that did not develop disease had not accumulated consensus changes in *env* and *nef* (Singh et al., 2001). These results suggested that *vpu*$SHIV_{KU\text{-}1bMC33}$ was less pathogenic than parental $SHIV_{KU\text{-}1bMC33}$ but that the virus could continue to evolve and accumulate amino acid changes within Env and/or Nef that compensated for the lack of a functional Vpu protein and attests to the plasticity of the retroviral genome. The importance of Vpu in the circulating $CD4^+$ T cell loss caused by SHIV was also demonstrated in a recent study of the entire *vpu* coding sequence prior to *env* (Stephens et al., 2002). Taken together, these studies indicate a role for the *vpu* gene product in SHIV and probably HIV-1 pathogenesis. Similar to the deletion of Vpu, deletion of other accessory genes, such as *nef* and/or *vpr*, from SIVmac results in viruses with attenuated pathogenicity (Daniel et al., 1992; Desrosiers et al. 1998) that may require longer periods of time to cause disease (Baba et al., 1995; Hofmann-Lehman et al., 2003). Both of these genes are considered to contribute to the pathogenicity of SIV and HIV-1. Similarly, we believe that deletion of the *vpu* gene results in an attenuated virus that in certain circumstances can evolve to compensate for the lack of this gene. Taken together, these results emphasize that pathogenicity caused by HIV-1, SIV, or SHIV is multigenic in nature and that Vpu contributes to the pathogenicity of SHIV and HIV-1.

In this report, we have analyzed the ability of the pathogenic molecular clone $SHIV_{KU\text{-}1bMC33}$ to cause rapid $CD4^+$ T cell loss and AIDS following site-directed changes that removed the two casein kinase II phosphorylation sites in the cytoplasmic domain of the Vpu protein. Using a VpuEGFP reporter system, we showed that the protein was localized to the same compartments as the unmodified protein, had a similar stability in cells, but was incapable of promoting CD4 degradation. We hypothesized that because of the importance of the casein kinase II sites to CD4

degradation by Vpu that the virus would be less pathogenic for macaques. We found that one of four macaques inoculated with $SHIV_{S52,56G}$ developed a rapid $CD4^+$ T cell loss that is typically observed with pathogenic SHIV, whereas all four macaques inoculated with the parental $SHIV_{KU\text{-}1bMC33}$ virus developed rapid $CD4^+$ T cell loss within 1 month which was maintained for up to 6 months postinoculation. These results indicate that the casein kinase II sites of the Vpu protein are important to the massive $CD4^+$ T cell loss associated with infection with this virus. The obvious question that arose from the results of this study was "Why did macaque CC8X develop severe $CD4^+$ T cell loss and die at 18 weeks postinoculation?" We hypothesized that the virus in this macaque may have selected for mutations in *vpu* that might have resulted in the reversion of the glycines at positions 52 and 56 to serine residues or compensating amino acid substitutions in other proteins, such as Env. Sequence analysis of bulk PCR that amplified *vpu* and individual *vpu* clones at different time points postinoculation was used to determine if there was a reversion of the glycine residues back to serines. The results of the bulk PCR sequencing indicate a reversion first at position 56 and later at position 52. While we were only able to detect the reversions beginning at 3 weeks in the PBMC, which was several weeks after the severe $CD4^+$ T cell loss occurred, the mutations that we observed in the PBMC may have followed what had occurred earlier in primary and secondary lymphoid tissues. Interestingly, the thymus contained only the input viral sequences, whereas the spleen and lymph nodes had a mixture of the viruses. Because these results were based on PCR amplification of the *vpu* genes from isolated DNA, we also analyzed the virus that was recovered from the mesenteric lymph nodes, spleen, thymus, and PBMC obtained at necropsy. Our results indicated that the reversions were present in infectious cytopathic viruses recovered from these tissues, providing additional evidence that selection for these mutations had occurred in macaque CC8X. The reversions observed in macaque CC8X are reminiscent of the changes that occurred in the derivation of a pathogenic variant from the original nonpathogenic SHIV-4 (Joag et al., 1996; Stephens et al., 1997; McCormick-Davis et al., 1998) and provide another example that a "functional Vpu" makes the pathogenic SHIV a more "fit" virus, possibly by giving such a virus a replicative advantage over other quasispecies in the same macaque lacking a functional Vpu. Taken together, the results of this study indicate for the first time that the phosphorylation of Vpu potentiates a dramatic loss in $CD4^+$ T cells following inoculation with pathogenic $SHIV_{KU\text{-}1bMC33}$ and provide additional evidence that this viral protein is important to the $CD4^+$ T cell loss in HIV-1-infected people. The results of this study also reinforce the utility of the $SHIV_{KU\text{-}1bMC33}$/pig-tailed macaque model for analyzing the role of various amino acids/domains in the Vpu in HIV-1 pathogenesis.

Materials and methods

Cells, plasmids, and viruses

The C8166 cell line was used as the indicator to measure the infectivity and cytopathicity of the viruses used in this study. C8166 cells were maintained in RPMI 1640, supplemented with 10 mM HEPES buffer, pH 7.3, 2 mM glutamine, 5 μg/ml of gentamicin, and 10% fetal bovine serum (R10FBS). The derivation of $SHIV_{KU\text{-}1bMC33}$ has been previously described (Narayan et al., 1999; McCormick-Davis et al., 2000b; Stephens et al., 2002).

Construction of VpuEGFP, $Vpu_{S52,56G}$EGFP, and EGFP expression vectors

In order to construct the VpuEGFP vector for expression studies, the *vpu* gene from $SHIV_{KU\text{-}1bMC33}$, which has a fully functional *vpu* gene, was amplified from infected cells using PCR and oligonucleotides 5′-TGTAATGCAACCTATACCAATAGTAGCA-3′ (sense strand, at the 5′ end of the gene) and 5′-TCCATGGGATCATCAACATCCCAAGTAGC-3′ (antisense and also containing an *Nco*I site). One microgram of genomic DNA was used in the PCR containing 1.4 mM $MgSO_4$, 200 M each of the four deoxynucleotide triphosphates, 100 pM each oligonucleotide primer, and a mixture of *Taq* and *Pyrococcus* species GB-D polymerases (Elongase, GibcoBRL). The template was denatured at 94°C for 2 min and PCR amplification performed with an automated DNA Thermal Cycler (Perkin–Elmer Cetus) for 35 cycles using the following profile: denaturation at 94°C for 30 s, annealing at 65°C for 1 min, and primer extension at 68°C for 5 min. Amplification was completed by incubation for 10 min at 68°C. The amplified fragment, which is approximately 250 bases in length, was cloned into the pGEM-T vector (Promega) according to the manufacturer's instructions. Recombinants were identified and inserts sequenced in their entirety to ensure that no sequence errors were introduced during the amplification process. This plasmid, known as p*vpu*NcoI, was digested to completion using the restriction endonuclease *Nco*I; the *vpu* gene fragment was gel purified and subcloned into *Nco*I-digested CIAP treated pEGFP vector (Clontech Laboratories; Cormack et al., 1996) that has an *Nco*I site at the 5′ end of the EGFP gene. The resulting plasmid, known as p*vpu*EGFP, was sequenced to ensure that (1) the *vpu* gene was inserted in the proper orientation and (b) the *vpu*/EGFP junction was in-frame. The *vpu*EGFP fusion gene was then inserted into the pcDNA3.1(+) vector for expression studies. The p*vpu*EGFP vector was digested to completion with *Kpn*I and *Stu*I, which cuts on either side of the insert. The insert was gel purified and subcloned into the pcDNA3.1(+), which was also digested with *Kpn*I and *Eco*RV. The resulting plasmid, pc*vpu*EGFP, contained the entire *vpu* gene fused to the gene for EGFP under the control of the CMV immediate early promoter. A similar

plasmid was constructed which expressed only the EGFP protein (pcEGFP).

To determine if VpuEGFP was phosphorylated, we altered the two serine residues that were previously reported to be phosphorylated by casein kinase II to glycine residues. This was performed using two rounds of mutagenesis. The oligonucleotide primers used in the first round were 5′-GAAAGAGCAGAAGACGGTGGCAATGAGAGTGAAG-3′ (sense) and 5′-CTTCACTCTCATTGCCACCGTCTTC-TGCTCTTTC-3′ (antisense), which changed the serine at position 52 to a glycine residue. In the second round of mutagenesis, the oligonucleotide primers used were 5′-GACG-GTGGCAATGAGGGTGAAGGAGAAATATC-3′ (sense) and 5′-GATATTTCTCCTTCACCCTCATTGCCACCGT-C-3′ (antisense), which changed the serine residue at position 56 to a glycine residue. The mutagenesis protocols were identical to those described above. A plasmid designated pc*vpu*$_{S52,56G}$EGFP was isolated and the VpuEGFP insert sequenced to ensure that the correct mutation was introduced and that no additional mutations were accidentally introduced. This insert was then inserted into the pcDNA3.1(+) vector as described above, designated pc*vpu*$_{S52,56G}$EGFP, and used in expression studies.

Transfection and intracellular location studies

VpuEGFP and other mutants were transfected in human 293 cells to assess their subcellular localization using a cationic polymer (polyethylenimine) transfection reagent (ExGen 500, MBI Fermentas) using the manufacturer's protocol. Briefly, 1–3 $\times$ 10^5 cells were seeded into each well of a six-well tissue culture plate 24 h prior to transfection. Transfection was carried out on cultures that were 50–60% confluent using 9.5 μg of plasmid DNA and 26 μl of ExGen 500 corresponding to 5 equivalents. Each plasmid sample and polyethylenimine were diluted in 75 μl of 150 mM sodium chloride solution separately. Samples were vortexed gently and immediately centrifuged at low revolution for a few seconds. Polyethylenimine was then added to the plasmid DNA solution, mixed with a vortex, and allowed to stand at room temperature for 10 min. The 293 cells were washed with serum-free media twice and added with 1.5 ml of serum-free DMEM. Polyethylenimine/DNA mixture was added to the cells and the plate swirled by slow hand rotation for a couple of seconds. Culture plates were centrifuged at 280 $\times$ *g* for 5 min and incubated at 37°C for 30 min. The medium from transfected cultures was replaced with fresh complete growth media and cells were incubated at 37°C in a 5% CO_2 atmosphere. Transfected cells were observed by confocal microscopy, which is known to have the advantage that fluorescence can be detected from cells in different layers. For confocal microscopy, 293 cells were plated and transfected on two-well Lab-Tek chamber slides. To prepare cells for detection of EGFP fluorescence, the medium was removed after 48 h following transfection, the monolayers were briefly rinsed in PBS, and the cells fixed for 10 min at room temperature in freshly prepared 1% paraformaldehyde in PBS. The upper chambers of the slides were removed and fixed cells were treated with Prolong Anti-Fade (Molecular Probes, Eugene, OR) and mounted under a coverslip. Images were collected using a Zeiss Confocal Laser Scanning Microscope, LSM-510, using an excitation wavelength of 488 nm with a LP-505 emission filter. Images were analyzed and three-dimensional reconstructions of the subcellular localization of the VpuEGFP mutants were generated using LSM-510 software.

CD4 staining

To determine if the VpuEGFP construct was capable of promoting degradation of CD4 in transfected cells, we employed HeLa $CD4^+$ cells. Briefly, HeLa $CD4^+$ cells were grown on coverslips and transfected with *pcvpu*EGFP as described earlier. At 48 h posttransfection, cells were washed twice with wash buffer (PBS, pH 7.2, containing 2% fetal calf serum and 0.01% NaN_3) and reacted with mouse anti-CD4 (clone SFCI12T4D11CD4, Beckman-Coulter, 1:500 dilution) for 45 min. After the incubation, coverslips were washed three times and incubated with rhodamine-conjugated secondary antibody (goat, Chemicon, 1:50 dilution) for 35 min followed by washing five times in buffer without serum. Cells were then fixed in 1% formalin for 10 min, washed twice, equilibrated with antifade buffer, and mounted on microscope glass slides using Anti-Fade (Molecular Probes). Cells were immediately observed under a fluorescent microscope (Nikon TE300) with a fluorescein filter (for visualization of EGFP) and rhodamine filters (for visualization of CD4 staining). All the staining procedures were performed on ice and in the dark. HeLa $CD4^+$ cells transfected with EGFP alone served as controls for down-regulation of CD4 and cultures of HeLa $CD4^+$ cells treated with wash buffer instead of primary antibody served as negative controls for CD4 staining. A minimum of 400 EGFP expressing cells were counted.

Construction of SHIV$_{S52,56G}$

A virus was constructed in which *vpu* was mutated such that the serines at positions 52 and 56 of Vpu were changed to glycine residues. Plasmid pUC19 SNvpu12, containing the *Sph*I to *Kpn*I fragment of SHIV$_{KU\text{-}1bMC33}$ in pUC-19 (and coding for the *tat, rev, vpu,* and 5′ end of *env*) was used for the site-directed mutagenesis studies, which were performed in two steps. In the first round of mutagenesis, oligonucleotides 5′-GAAAGAGCAGAAGACGGTGGCA-ATGAGAGTGAA-3′ (sense) and 5′-CTTCACTCTCATT-GCCACCGTCTTCTGCTCTTTC-3′ (antisense) were used to change the serine at position 52 to a glycine residue. The plasmid used was pUC19 SNvpu12 with the Quick-Change Mutagenesis Kit (Stratagene) according to the manufacturer's instructions. In the second round of mutagenesis, oligonucleotides 5′-GACGGTGGCAATGAGGGTGAAG-

GAGAAATATC-3′ (sense) and 5′-GATATTTCTCCTTC-ACCCTCATTGCCACCGTC-3′ (antisense) were used to change the serine at position 56 to a glycine. Clones and plasmids were isolated and the entire insert was sequenced to determine if the mutations were introduced as expected and to ensure that no additional changes were introduced during the mutagenesis step. A plasmid was isolated and designated $pvpu_{S52,56G}$ that contained the desired mutations. This plasmid was digested to completion with *Sph*I/*Kpn*I, and the 450-bp fragment isolated and subcloned into the $p3'SHIV_{KU\text{-}1bMC33}$ plasmid as previously described (McCormick-Davis et al., 2000b). The resulting plasmid, $p3'SHIV_{S52,56G}$, was used to construct an infectious virus known as $SHIV_{S52,56G}$ using procedures previously described (Stephens et al., 1998; Liu et al., 1999; McCormick-Davis et al., 2000b; Singh et al., 2002). Stocks of the virus were prepared and titered in C8166 cells. The virus stock was examined by PCR amplification of the *vpu* gene sequence and sequence analysis to ensure the purity of the stock virus. We also sequenced the *tat*, *rev*, *env*, and *nef* genes to ensure that they were identical to the parental $SHIV_{KU\text{-}1bMC33}$ sequence.

p27 assays

Standard p27 assays were used to assess release of viral particles from cells infected with $SHIV_{S52,56G}$ or parental $SHIV_{KU\text{-}1bMC33}$. Cultures of 10^6 C8166 cells were inoculated with equivalent amounts (30 ng) of cell-free virus stocks for 2 h. At the end of 2 h the cells were centrifuged at $400 \times g$ for 10 min and the pellet was washed with 10 ml of medium. This was repeated two additional times. The cells were resuspended in RPMI 1640 supplemented with 10% FBS and antibiotics and this was considered the 0 time point of the assay. Cultures were incubated at 37°C and aliquots of the culture were removed at 0, 1, 3, 5, 7, and 10 days. The culture medium was separated from the cells by centrifugation and then assayed for p27 according to the manufacturer's instructions.

Macaques analyzed in this study

Four pig-tailed macaques (CC8X, CC8V, P003, and P017) were inoculated intravenously with 1 ml of undiluted supernatant from C8166-grown stocks of $SHIV_{S52,56G}$ containing approximately 10^4 $TCID_{50}$/ml as previously described (McCormick-Davis et al., 2000b). At 4 months postinoculation, macaque CC8X became anemic (hemoglobin 5.7 g/dl, mean cell packed volume of 18%), developed thrombocytopenia (28,000 per/liter) and pectaheal hemorrhages, and was euthanized in a moribund condition at 18 weeks postinoculation. Macaque CC8V did not develop significant $CD4^+$ T cell loss and was sacrificed at 9 months in a healthy condition with normal $CD4^+$ T cell counts for examination of virus burdens. Macaque P003 developed a wasting condition starting at 10 months postinoculation and was subsequently euthanized at 11 months postinoculation. Macaque P017 maintained circulating $CD4^+$ T cell levels in the normal range and was euthanized in a heathly condition 12 months postinoculation. Four additional macaques (2000, 2001, CM4G, and CM4K) were inoculated with 1 ml of parental $SHIV_{KU\text{-}1bMC33}$ (10^4 $TCID_{50}$) and circulating $CD4^+$ T cell counts followed for at least 6 months. Macaques CM4G and CM4K were euthanized at 6 months after inoculation and analyzed for virus content and SHIV-associated pathology.

Processing of blood samples

PBMC were prepared by centrifugation on Ficoll–Hypaque gradients as described previously (Joag et al., 1996). Tenfold dilutions of PBMC (10^6 cells/ml) were inoculated into replicate cultures of C8166 cells in 24-well plates and the cocultures examined for development of cytopathic effects as previously described (McCormick-Davis et al., 2000b). Infectivity titers in plasma were reported as $TCID_{50}$/ml and cells producing infectious cytopathic virus in the blood reported as the number of infected cells/10^6 PBMC. Alterations in $CD4^+$ and $CD8^+$ T lymphocytes after experimental inoculations were monitored sequentially by FACS analysis (Becton–Dickinson). T lymphocyte subsets were labeled with OKT4 (CD4; Ortho Diagnostics Systems, Inc.), B9.11 (CD8; Coulter Immunology), and SP34 (CD3; Pharmingen), or FN18 (CD3; Biosource International) monoclonal antibodies.

Processing of tissue samples at necropsy

At the time of euthanasia, all animals in this study were anesthetized by administration of 10 mg/kg of ketamine (im) followed by an intravenous administration of sodium pentobarbital at 20–30 mg/kg. A laparotomy was performed and the animal exsanguinated by aortic canulation. The chest was opened, the left ventricle canulated, the right atrium nicked, and the animal perfused with 1 liter of cold pyrogen-free Ringer's saline. All aspects of the animal studies were performed according to the institutional guidelines for animal care and use at University of Kansas Medical Center. At necropsy, tissues from the axillary lymph nodes, heart, kidney, liver, lungs, mesenteric lymph nodes, pancreas, small intestine, spleen, and thymus were fixed in 10% neutral buffered formalin and embedded in paraffin. Sections (5 μm) were stained with hematoxylin and eosin for routine histological examination. In addition, the right halves of the brain and spinal cord were dissected into frontal, motor, parietal, temporal, and occipital cortices; the corpus callosum, thalamus, basal ganglia, midbrain, pons, medulla, cerebellum, and cervical, thoracic, and lumbar spinal cord were also processed as above. Portions of each

of the visceral organs and the CNS were also frozen in liquid nitrogen for molecular virological analysis.

PCR amplification and sequence analysis of vpu, env, and nef sequences

Because potential reversion of the glycine residues at positions 52 and 56 to serine residues may have occurred following inoculation with $SHIV_{S5256G}$ or mutations may have occurred in other genes, such as *env* and *nef*, that compensated for the loss of Vpu function, we analyzed *vpu*, *env*, and *nef* sequences at different times following inoculation of macaque CC8X with $SHIV_{S52,56G}$ and compared these sequences to those from $SHIV_{KU\text{-}1bMC33}$. PBMC were collected at 3, 8, 12, and 18 weeks (necropsy) after inoculation and DNA extracted as previously described (McCormick-Davis et al., 2000b). For analysis of *vpu* and gp120 sequences, oligonucleotide primers 5′-CCTAGACTAGAGCCCTGGAAGCATCC-3′ and 5′-AGTGCTTCCTGCTGCTCCCAAGAACCC-3′ were used, which are complementary to nucleotides 5845 to 5870 and 7781 to 7810 of the HIV-1 (HXB2) genome (Ratner et al., 1985), respectively. One microgram of genomic DNA was used in the PCR (Saiki et al., 1985, 1988) containing 1.4 mM $MgSO_4$, 200 M each of the four deoxynucleotide triphosphates, 100 pM each oligonucleotide primer, and a mixture of *Taq* and *Pyrococcus* species GB-D polymerases (Elongase, Gibco-BRL). The template was denatured at 94°C for 2 min and PCR amplification performed with an automated DNA Thermal Cycler (Perkin–Elmer Cetus) for 35 cycles using the following profile: denaturation at 94°C for 30 s, annealing at 65°C for 1 min, and primer extension at 68°C for 5 min. Amplification was completed by incubation for 10 min at 68°C. Three separate PCRs were performed for each region of viral genome that was studied. The amplified products from three separate reactions were separated by electrophoresis in a 1% agarose gel, isolated, and molecularly cloned into the pGEM-T Easy vector according to the manufacturer's instructions. Cycle sequencing reactions using the BigDye Terminator Cycle sequencing Ready Reaction kit with AmpliTaq DNA polymerase, FS (PE Applied Biosystems, Foster City, CA) and sequence detection was conducted with an Applied Biosystems 377 Prism XL automated DNA sequencer and visualized using the ABI Editview program.

For amplification of *nef*, oligonucleotide primers 5′-CCACATACCTAGAAGAATAAGACAGGG-3′ (sense) and 5′-ACATCCCCTTGTGGAAAGTCCCTGCTGTTT-3′ (antisense) were used, which are complementary to nucleotides 8746 to 8772 of the HIV-1 (HXB2) genome (Ratner et al., 1985) and 9868 to 9898 of the $SIV_{mac}239$ genome (Regier and Desrosiers, 1990), respectively. The conditions for amplification, cloning, and sequencing of the PCR products were as described above.

PCR analysis of tissues for the presence of viral sequences

SHIV gag

Visceral organs (ileum, lymph nodes, spleen, lung, liver, and thymus) were collected and DNA was isolated as described below. The brain and spinal cord from infected macaques CC8X, CC8V, P017, and P003 were taken at necropsy and dissected into the following regions: frontal cortex, parietal cortex, occipital cortex, motor cortex, temporal cortex, corpus callosum thalamus, basal ganglia, midbrain, pons, medulla, cerebellum, cervical spinal cord, thoracic spinal cord, and lumbar spinal cord. The tissues were homogenized in a tight-fitting Dounce homogenizer in the presence of TE buffer (50 mM Tris–HCl, pH, 8.2, 10 mM EDTA) and 0.5% SDS. The homogenate was digested at 37°C for 2 h in the presence of 100 μg/ml of proteinase K followed by extraction twice with an equal volume of phenol and once with chloroform:isoamyl alcohol. The DNA in the aqueous phase was precipitated with 2 vol of ethanol, pelleted, and resuspended in DNase-free H_2O. We used nested PCR to determine if SIV *gag* sequences were present in the DNA isolated from the various tissues (Joag et al., 1994). In the first round, the SIV oligonucleotide primers used were 5′-GATGGGCGTGAGAAACTCCGTCTT-3′ (sense) and 5′-CCTCCTCTGCCGCTAGATGGTGCTGTTG-3′ (antisense), which are complementary to bases 1052 to 1075 and 1423 to 1450 of the $SIV_{mac}239$ *gag* gene, respectively (Regier and Desrosiers, 1990). As an internal control, separate PCRs were performed in which the fourth exon of β-actin was amplified with oligonucleotide primers 5′-TCATGTTTGAGACCTTCAACACCCCAG-5′(sense) and 5′-CCAGGAAGGAAGGCTGGAAGAGTGCC-5′ (antisense) complementary to the published sequence (Nakijima-Iijima et al., 1985). The PCR amplification was performed using the following conditions: denaturation at 92°C for 1 min; annealing at 55°C for 1 min; and primer extension at 72°C for 3 min. To increase the sensitivity of the reaction, 1 μl of the first PCR product was used as a template for a second amplification using the same conditions. The nested SIV primers used were 5′-GTACATGTTGAAGCATGTAGTATGGGCAGC-3′ (sense) and 5′-CACCACTAGGTGTCTCTGCACTATGTGTTTTGC-3′ (antisense). The nested β-actin primers used were 5′-CCCCAGCCATGTACGTTGCTATCC-3′ (sense) and 5′-GCCTCAGGGCAGCGGAACCGCTCA-3′ (antisense). Samples were amplified for another 35 cycles as described above. Following the second round of amplification, a 10-μl aliquot was removed and run on a 1.5% agarose gel and bands were visualized by staining with ethidium bromide.

Detection of SHIV long terminal repeat (LTR) circles

Examination of 2-LTR circular DNA provides a view of a spreading infection based on a viral DNA form that is structurally distinct and known to have a short half life in

infected cells (Pauza et al., 1994; Zazzi et al., 1997; Teo et al., 1997; Sharkey et al., 2000; Sharkey and Stevenson, 2001). We analyzed the DNA isolated from PBMC, ileum, liver, lymph node, lung, and spleen and the 14–15 regions of the CNS for the presence of 2-LTR circular forms of DNA as previously described (McCormick-Davis et al., 2000b). The oligonucleotides used in the first round were 5′-ATTTCGCTCTGTATTCAGTCGCTCTGC-3′ (U5 region) and 5′-CCTCCTGTGCCTCATCTGATACATTTA-C-3′ (U3 region), which correspond to bases 10335 to 10361 and 180 to 153 of the SHIV genome, respectively. The PCR amplification was performed using the following conditions: denaturation at 92°C for 1 min; annealing at 55°C for 1 min; and primer extension at 72°C for 3 min. One microliter of the first PCR product was used as a template for a second amplification using the same conditions. The oligonucleotide primers used for the second round were 5′-AGGTTCTCTCCAGCACTAGCAGGTAG-AGC-3′ (U5 region) 5′-TTGGGTATCTAATTCCTGGTC-CTGAG-3′ (U3 region; opposite strand; 456), which correspond to bases 10389 to 10417 and 120 to 95 of the SHIV genome, respectively. Samples were amplified for another 35 cycles as described above. Following the second round of amplification, a 10-μl aliquot was removed and run on a 1.5% agarose gel and bands were visualized by staining with ethidium bromide. The predicted product of the 2-LTR PCR product is 361 bp.

Analysis of virus loads in macaques

PCR–ICA

The virus loads in the lymphoid tissues (spleen, lymph nodes, thymus, PBMC) were determined using a quantitative PCR assay modified from a PCR-infected cell assay previously described (Joag et al., 1994; Stephens et al., 1998). In this assay, 1 μg of total cellular DNA isolated from tissues was subjected to a series of 10-fold dilutions such that samples contained from 100 ng to 10 fg (less than one copy of chromosomal DNA). These samples were used in nested PCR reactions that amplified either the β-actin gene of the cell (a single copy gene) or the *gag* gene from $SIV_{mac}239$. Amplification of either gene using the primers previously described was shown to detect one copy of each gene (Joag et al., 1994). Thus amplification of the β-actin gene determined the number of genome equivalents in each sample, while amplification with the *gag* primers determined the number of viral copies per number of genome equivalents. The values were expressed as the number of viral copies per 10^6 genome equivalents.

Plasma virus RNA loads

Plasma viral RNA loads were determined on RNA extracted from 500 liters of EDTA -treated plasma. Virus was pelleted and RNA extracted using the Qiagen viral RNA kit (Qiagen, Valencia, CA). RNA samples were analyzed by real-time RT–PCR using *gag* primers and a 5′FAM- and 3′TAMRA-labeled Taqman probe that was homologous to the SIV *gag* gene as previously described (Hofman-Lehmann et al., 2000). Standard curves were prepared using a series of six 10-fold dilutions of viral RNA of known concentration. The sensitivity of the assay was 100 RNA equivalents/ml. Samples were analyzed in triplicate and the numbers of RNA equivalents were calculated per milliliter of plasma.

Acknowledgments

The work reported here is supported by NIH Grants MH61230 and AI51981 to E.B.S. and CA75922 and RR00163 to S.W.W.

References

Baba, T.W., Jeong, Y.S., Pennick, D., Bronson, R., Greene, M.F., Ruprecht, R.M., 1995. Pathogenicity of live, attenuated SIV after mucosal infection of neonatal macaques. Science 267, 1820–1825.

Daniel, M.D., Kirchhoff, F., Czajak, S.C., Sehgal, P.K., Desrosiers, R.C., 1992. Protective effects of a live attenuated SIV vaccine with a deletion in the nef gene. Science 258, 1938–1941.

Desrosiers, R.C., 1998. Prospects for live attenuated HIV. Nature Med. 4, 982.

Ewart, G.D., Sutherland, T., Gage, P.W., Cox, G.B., 1996. The Vpu protein of human immunodeficiency virus type 1 forms cation- selective ion channels. J. Virol. 70, 7108–7115.

Fujita, K., Omura, S., Silver, J., 1997. Rapid degradation of CD4 in cells expressing human immunodeficiency virus type 1 Env and Vpu is blocked by proteasome inhibitors. J. Gen. Virol. 78, 619–625.

Hofmann-Lehmann, R, Swenerton, R.K., Liska, V., Leutenegger, C.M., Lutz, H., McClure, H.M., Ruprecht, R.M., 2000. Sensitive and robust one-tube real-time reverse transcriptase–polymerase chain reaction to quantify SIV RNA load: comparison of one- versus two-enzyme systems. AIDS Res. Hum. Retroviruses 16, 1247–1257.

Hofmann-Lehmann, R., Vlasak, J., Williams, A.L., Chenine, A.L., McClure, H.M., Anderson, D.C., O'Neil, S., Ruprecht, R.M., 2003. Live attenuated, nef-deleted SIV is pathogenic in most adult macaques after prolonged observation. AIDS 17, 156–166.

Joag, S.V., Stephens, E.B., Adams, R.J., Foresman, L., Narayan, O., 1994. Pathogenesis of SIVmac infection in Chinese and Indian rhesus macaques: effects of splenectomy on virus burden. Virology 200, 436–446.

Joag, S.V., Li, Z., Foresman, L., Stephens, E.B., Zhao, L.-J., Adany, I., Pinson, D.M., McClure, H.M., Narayan, O., 1996. Chimeric simian/human immunodeficiency virus that causes progressive loss of CD4+ T cells and AIDS in pig-tailed macaques. J. Virol. 70, 3189–3197.

Karlsson, G.B., Halloran, M., Li, J., Park, I.W., Gomila, R., Reimann, K.A., Axthelm, M.K., Iliff, S.A., Letvin, N.L., Sodroski, J., 1997. Characterization of molecularly cloned simian-human immunodeficiency viruses causing rapid CD4+ lymphocyte depletion in rhesus monkeys. J. Virol. 71, 4218–4225.

Liu, Z.Q., Muhkerjee, S., Sahni, M., McCormick, D.C., Leung, K., Li, Z., Gattone, V.H., Tian, C., Doms, R.W., Hoffman, T.L., Raghavan, R., Narayan, O., Stephens, E.B., 1999. Derivation and biological characterization of a molecular clone of SHIV(KU-2) that causes AIDS, neurological disease, and renal disease in rhesus macaques. Virology 260, 295–307.

Luciw, P.A., Mandell, C.P., Himathongkham, S., Li, J., Low, T.A., Schmidt, K.A., Shaw, K.E., Cheng-Mayer, C., 1999. Fatal immuno-

pathogenesis by SIV/HIV-1 (SHIV) containing a variant form of the HIV-1SF33 env gene in juvenile and newborn rhesus macaques. Virology 263, 112–127.

Maldarelli, F., Chen, M.Y., Willey, R.L., Strebel, K., 1993. Human immunodeficiency virus type 1 Vpu protein is an oligomeric type I integral membrane protein. J. Virol. 67, 5056–5061.

McCormick-Davis, C., Dalton, S.B., Singh, D.K., Stephens, E.B., 2000a. Comparison of Vpu sequences from diverse geographical isolates of HIV type 1 identifies the presence of highly variable domains, additional invariant amino acids, and a signature sequence motif common to subtype C isolates. AIDS Res. Hum. Retroviruses 16, 1089–1095.

McCormick-Davis, C., Dalton, S.B., Hout, D.R., Singh, D.K., Berman, N.E., Yong, C., Pinson, D.M., Foresman, L., Stephens, E.B., 2000b. A molecular clone of simian-human immunodeficiency virus (ΔVpuSHIV$_{KU1bMC33}$) with a truncated, non-membrane-bound vpu results in rapid CD4(+) T cell loss and neuro-AIDS in pig-tailed macaques. Virology 272, 112–126.

Nakijima-Iijima, S., Hamada, H., Reddy, P., Kakunaga, T., 1985. Molecular structure of the human cytoplamic beta-actin gene:interspecies homology of sequences in the intron. Proc. Natl. Acad. Sci. USA 82, 6133–6137.

Narayan, S.V., Mukherjee, S., Jia, F., Li, Z., Wang, C., Foresman, L., McCormick, D.C., Stephens, E.B., Joag, S.V., Narayan, O., 1999. Characterization of a neutralization-escape variant of SHIVKU-1, a virus that causes acquired immune deficiency syndrome in pig-tailed macaques. Virology 256, 54–63.

Paul, M., Jabbar, M. A., 1997. Phosphorylation of both phosphoacceptor sites in the HIV-1 Vpu cytoplasmic domain is essential for Vpu-mediated ER degradation of CD4. Virology 232, 207–216.

Paul, M., Mazumder, S., Raja, N., Jabbar, M.A., 1998. Mutational analysis of the human immunodeficiency virus type 1 Vpu transmembrane domain that promotes the enhanced release of virus-like particles from the plasma membrane of mammalian cells. J. Virol. 72, 1270–1279.

Pauza, C.D., Trivedi, P., McKechnie, T.S., Richman, D.D., Graziano, F.M., 1994. 2-LTR circular viral DNA as a marker for human immunodeficiency virus type 1 infection in vivo. Virology 205, 470–478.

Raja, N.U., Jabbar, M.A., 1997. The human immunodeficiency virus type 1 Vpu protein tethered to the CD4 extracellular domain is localized to the plasma membrane and is biologically active in the secretory pathway of mammalian cells: implications for the mechanisms of Vpu function. Virology 220, 141–151.

Ratner, L., Haseltine, W., Patarca, R., Livak, K.J., Starcich, B., Josephs, S.F., Doran, E.R., Rafalski, J.A., Whitehorn, E.A., Baumeister, K., 1985. Complete nucleotide sequence of the AIDS virus, HTLV-III. Nature 313, 277–284.

Regier, D.A., Desrosiers, R.C., 1990. The complete nucleotide sequence of a pathogenic molecular clone of simian immunodeficiency virus. AIDS Res. Hum. Retroviruses 6, 1221–1231.

Reimann, K.A., Li, J.T., Voss, G., Lekutis, C., Tenner-Racz, K., Racz, P., Lin, W., Montefiori, D.C., Lee-Parritz, D.E., Lu, Y., Collman, R.G., Sodroski, J., Letvin, N.L., 1996. An env gene derived from a primary human immunodeficiency virus type 1 isolate confers high in vivo replicative capacity to a chimeric simian/human immunodeficiency virus in rhesus monkeys. J. Virol. 70, 3198–3206.

Saiki, R.K., Scharf, S., Faloona, F., Mullis, K.B., Horn, G.T., Erlich, H.A., Amheim, N., 1985. Enzymatic amplification of β-globin genomic sequences and restriction site analysis for diagnosis of sickle cell anemia. Science 230, 1350–1354.

Saiki, R.K., Gelfand, D.H., Stoffel, S., Scharf, S.J., Higuchi, R., Horn, G.T., Mullis, K.B., Erlich, H.A., 1988. Primer-directed enzymatic amplification of DNA with a thermostable DNA polymerase. Science 239, 487–491.

Sansom, M.S., Forrest, L.R., Bull, R., 1998. Viral ion channels: molecular modeling and simulation. Bioessays 20, 992–1000.

Schubert, U., Henklein, P., Boldyreff, B., Wingender, E., Strebel, K., Porstmann, T., 1994. The human immunodeficiency virus type 1 encoded Vpu protein is phosphorylated by casein kinase-2 (CK-2) at positions Ser52 and Ser56 within a predicted alpha-helix-tum-alpha-helix-motif. J. Mol. Biol. 236, 16–25.

Schubert, U., Bour, S., Ferrier-Montiel, A.V., Montal, M., Maldarelli, F., Strebel, K., 1996a. The two biological activities of human immunodeficiency virus type 1 Vpu protein involve two separable structural domains. J. Virol. 70, 809–819.

Schubert, U., Ferrier-Montiel, A.V., Oblatt-Montal, M., Henklein, P., Strebel, K., Montal, M., 1996b. Identification of an ion channel activity of the Vpu transmembrane domain and its involvement in the regulation of virus release from HIV-1-infected cells. FEBS Letters 398, 12–18.

Schwartz, S., Felber, B.K., Fenyo, E.M., Pavlakis, G.N., 1990. Env and Vpu proteins of human immunodeficiency virus type 1 are produced from multiple bicistronic mRNAs. J. Virol. 64, 5448–5456.

Sharkey, M.E., Teo, I., Greenough, T., Sharova, N., Luzuriaga, K., Sullivan, J.L., Bucy, R.P., Kostrikis, L.G., Haase, A., Veryard, C., Davaro, R.E., Cheeseman, S.H., Daly, J.S., Bova, C., Ellison III, R.T., Mady, B., Lai, K.K., Moyle, G., Nelson, M., Gazzard, B., Shaunak, S., Stevenson, M., 2000. Persistence of episomal HIV-1 infection intermediates in patients on highly active anti-retroviral therapy. Nature Med. 6, 76–81.

Sharkey, M.E., Stevenson, M., 2001. Two long terminal repeat circles and persistent HIV-1 replication. Curr. Opin. Infect. Dis. 14, 5–11.

Singh, D.K., McCormick, C., Pacyniak, E., Lawrence, K., Dalton, S.B., Pinson, D.M., Sun, F., Berman, N.E., Calvert, M., Gunderson, R.S., Wong, S.W., Stephens, E.B., 2001. A simian human immunodeficiency virus with a nonfunctional Vpu (ΔvpuSHIV$_{KU-1bMC33}$) isolated from a macaque with neuroAIDS has selected for mutations in *env* and *nef* that contributed to its pathogenic phenotype. Virology 282, 123–140.

Stephens, E.B., Sahni, M., Leung, K., Raghavan, R., Joag, S.V., Narayan, O., 1998. Nucleotide substitutions in the long terminal repeat are not required for development of neurovirulence by simian immunodeficiency virus strain mac. J. Gen. Virol. 79, 1089–1100.

Stephens, E.B., McCormick, C., Pacyniak, E., Griffin, D., Pinson, D.M., Sun, F., Nothnick, W., Wong, S.W., Gunderson, R., Berman, N.E., Singh, D.K., 2002. Deletion of the *vpu* sequences prior to the *env* in a simian-human immunodeficiency virus results in enhanced Env precursor synthesis but is less pathogenic for pig-tailed macaques. Virology 293, 252–261.

Teo, I., Veryard, C., Barnes, H., An, S.F., Jones, M., Lantos, P.L., Luthert, P., Shaunak, S., 1997. Circular forms of unintegrated human immunodeficiency virus type 1 DNA and high levels of viral protein expression: association with dementia and multinucleated giant cells in the brains of patients with AIDS. Virol. 71, 2928–2933.

Willey, R.L., Maldarelli, F., Martin, M.A., Strebel, K., 1992. Human immunodeficiency virus type 1 Vpu protein induces rapid degradation of CD4. J. Virol. 66, 7193–7200.

Zazzi, M., Romano, L., Catucci, M., Venturi, G., De Milito, A., Almi, P., Gonnelli, A., Rubino, M., Occhini, U., Valensin, P.E., 1997. Evaluation of the presence of 2-LTR HIV-1 unintegrated DNA as a simple molecular predictor of disease progression. J. Med. Virol. 52, 20–25.